

Combining Amide-Proton-Transfer MRI with DCE-MRI to Improve Prostate Cancer Detection

G. Jia¹, R. Abaza², J. D. Williams³, D. L. Zynger³, J. Zhou⁴, Z. K. Shah¹, M. Patel¹, S. Sammet¹, L. Wei⁵, R. R. Bahnsen², and M. V. Knopp¹

¹Wright Center of Innovation in Biomedical Imaging and Department of Radiology, The Ohio State University, Columbus, OH, United States, ²Department of Urology, The Ohio State University, Columbus, OH, United States, ³Department of Pathology, The Ohio State University, Columbus, OH, United States, ⁴Department of Radiology, Johns Hopkins University, Baltimore, MD, United States, ⁵Center for Biostatistics, The Ohio State University, Columbus, OH, United States

Introduction

Amide-proton-transfer MRI has recently emerged as a new molecular-MRI technique in which the contrast is determined by a change in water intensity due to chemical exchange with saturated amide protons in protein backbones [1, 2]. This study is to evaluate whether APT-MRI can improve prostate cancer detection in addition to DCE-MRI.

Material and methods

Subjects Twelve patients with prostate cancer scheduled for prostatectomy were evaluated in the retrospective study. The mean age of the patients was 58.5 years (range, 47-68 years).

APT-MRI All patients were imaged on a 3 Tesla MR system (Achieva, Philips Healthcare, Cleveland, OH) using a 32-channel phased array coil. APT-MR imaging was based on single-slice single-shot TSE. The saturation pre-pulse was composed of a train of sixteen 180° block pulses, each with a pulse length of 31 ms and saturation amplitude of 161.3 Hz (3.8 μ T). Magnetization transfer spectra with 33 different frequency offsets (-8 to 8 ppm, interval 0.5 ppm) were acquired in three transverse slices at the apex, middle, and base section of the prostate.

DCE-MRI DCE-MRI was performed using a 3D T1-weighted fast field echo sequence in the axial plane with a temporal resolution of 10.7 sec/volume. The extracellular Gd-based contrast agent was intravenously injected (injection dose = 0.1 mmol/kg bodyweight, injection rate = 0.5 ml/sec) followed by a 20 ml saline flush at a rate of 2 ml/sec.

Image Processing After field inhomogeneity correction, APT-MR imaging was quantified using the APT ratio (APTR), which is associated with the magnetization transfer ratio asymmetry at 3.5 ppm. For DCE-MRI data analysis, regions of interest (ROIs) were drawn on tumor and benign peripheral zone (PZ) tissues. Tofts and Kermode pharmacokinetic model was used to fit the data on a pixel-by-pixel basis as well as the ROIs. K^{trans} (min^{-1}) and k_{ep} (min^{-1}) were calculated. The cutoff value was defined as the average of benign PZ tissue plus one standard deviation and used to differentiate tumor from benign PZ tissue.

Results

DCE-MRI was acquired in eleven out of twelve patients due to one patient (Patient F) allergic to Gd-based agent. K^{trans} was $0.50 \pm 0.23 \text{ min}^{-1}$ in tumor and $0.27 \pm 0.16 \text{ min}^{-1}$ in benign PZ ($P = 0.02$); and k_{ep} was $1.08 \pm 0.36 \text{ min}^{-1}$ in tumor and $0.56 \pm 0.25 \text{ min}^{-1}$ in benign PZ ($P = 0.001$). APTR in prostate cancer ROIs was $5.8\% \pm 3.2\%$, significantly higher than that in the peripheral zone benign regions ($0.3\% \pm 3.2\%$, $P = 0.006$; Figure 1). Using the cutoff value of K^{trans} (0.43 min^{-1}) and k_{ep} (0.71 min^{-1}), tumor and benign PZ cannot be discriminated in 3 cases (Patient D, I and K). The cutoff value of APTR (3.4%) can be used to differentiate tumor from benign PZ regions in the 3 cases and Patient F without DCE-MRI.

Discussions and Conclusion

APT-MR imaging provides unique information about the presence of prostate cancer based on increased cellular content of mobile proteins, which is complementary to DCE-MRI. Patient with impaired renal function is not uncommon in prostate cancer disease. APT-MRI can detect prostate cancer without injection of a contrast agent in order to improve the diagnostic ability of MRI. In conclusion, APT-MRI is capable to improve cancer detection in addition to microcirculation imaging.

References

1. Zhou J, et al. Magn Reson Med. 2004 May;51(5):945-52.
2. van Zijl PC, et al. PNAS. 2007 Mar 13;104(11):4359-64.

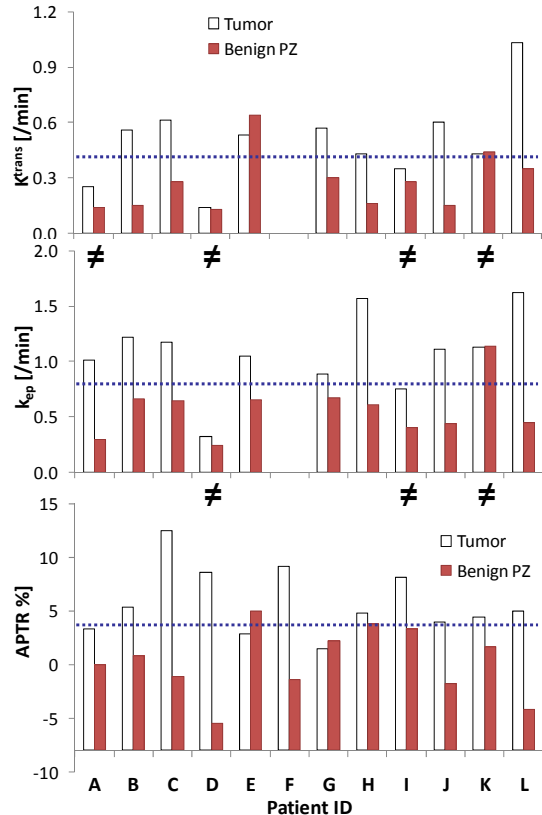


Figure 1. Histograms of K^{trans} , k_{ep} and APTR. By defining the cutoff value as 0.7 min^{-1} for k_{ep} , tumor and benign PZ cannot be discriminated in 3 cases (Patient D, I and K marked with ≠). No DCE-MRI was acquired in Patient F due to allergic to Gd-based agent. By defining APTR cutoff value of 3.4% , tumor and benign PZ regions in the 4 cases can be discriminated.

Figure 2. Patient K with a tumor in the left PZ. Tumor cannot be differentiated from benign PZ in K^{trans} and k_{ep} maps. APT-MRI shows higher APTR value in tumor than in benign PZ.

